Monopolar flocking of microtubules in collective motion

Farhana Afroze[1$], Daisuke Inoue[2$], Tamanna Ishrat Farhana[1], Tetsuya Hiraiwa[3,4], Ryo Akiyama[5], Arif Md. Rashedul Kabir[6], Kazuki Sada[1,6] and Akira Kakugo[1,6*]

1.Graduate School of Chemical Sciences and Engineering, Hokkaido University, Sapporo 060-0810, Hokkaido, Japan

2. Faculty of Design, Kyushu University, Fukuoka 815-8540, Japan

3. Mechanobiology Institute, National University of Singapore, Singapore 117411, Singapore

4. Universal Biology Institute, The University of Tokyo, Hongo, Tokyo 113-0033, Japan.

5. Department of Chemistry, Kyushu University, Fukuoka 819-0395, Japan

6. Faculty of Science, Hokkaido University, Sapporo 060-0810, Hokkaido, Japan

[$] These authors are contributed equally to this work.

Abstract

Flocking is a fascinating coordinated behavior of living organisms or self-propelled particles (SPPs). Particularly, monopolar flocking has been attractive due to its potential applications in various fields. However, the underlying mechanism behind flocking and emergence of monopolar motion in flocking of SPPs has remained obscured. Here, we demonstrate monopolar flocking of kinesin-driven microtubules, a self-propelled biomolecular motor system. Microtubules with an intrinsic structural chirality preferentially move towards counter-clockwise direction. At high density, the CCW motion of microtubules facilitates monopolar flocking and formation of a spiral pattern. The monopolar flocking of microtubules is accounted for by a torque generated when the motion of microtubules was obstructed due to collisions. Our results shed light on flocking and emergence of monopolar motion in flocking of chiral active matters. This work will help regulate the polarity in collective motion of SPPs which in turn will widen their applications in nanotechnology, materials science and engineering.

Keywords: Flocking, Collective motion, Pattern formation, Chirality, Polarity, Active matter

Introduction

Flocking is a typical example of collective motion which is exhibited by living organisms ranging from animals to bacteria [1-4], as well as artificial self-propelled particles (SPPs) [5-20]. One of the remarkable features of flocking is the emergence of ordered states in which the organisms or SPPs translocate towards the same direction and ultimately form a monopolar phase. Such unidirectional alignment of flocks (monopolar flocks) in collective motion has attracted much attention not only in non-equilibrium physics and biology but also in materials science and engineering. For instance, SPPs have been promising for potential applications in molecular transport systems and micro-devices, [21-25] where integration of the motion of SPPs is essential for efficient accomplishment of tasks and force integration. Several attempts were undertaken to align SPPs by using external stimuli or microfluidic channels [21-25]. Another approach was based on the application of ratcheting structures into systems that enabled collective works from randomly moving SPPs [26]. Monopolar flocking may offer advantages to integrate the motion of SPPs without application of these external stimuli. Despite such potential applications of flocking, the underlying mechanism of flocking and monopolar phase formation by flocks have remained obscured yet.

To investigate the mechanism of flocking in laboratory conditions, various wet experiments have been proposed using self-propelled colloids [5-9] and cytoskeletal protein filaments (actin, microtubules) driven by biomolecular motors [10-20]. In these works, the SPPs were often organized into monopolar flocks, similar to that observed in nature, depending on the density of the SPPs. However, microtubules driven by the biomolecular motor kinesin or dynein did not form monopolar flocks but exhibited collective motion with bipolar orientation [11, 17-20]. Recently we demonstrated an *in silico* study in which the SPPs had intrinsic chirality in their motion. The results of our simulation suggested that the SPPs with chiral motion facilitate monopolar and rotational flocking [27]. Inspired by the outcomes of our *in silico* work, in this study, we investigate the effect of chirality in motion of the kinesin-driven microtubules on their collective motion.

In order to demonstrate collective motion of the microtubules with innate chirality in their structure, we prepared the microtubules through polymerization of tubulin using the nucleotide guanylyl- (α, β)-methylene-diphosphonate (GMPCPP). GMPCPP is an analogue of guanosine triphosphate

(GTP) and predominantly polymerize microtubules by assembling 14-protofilaments (PFs) of tubulins in a left-handed supertwist helical alignment [28]. Since, while translocating along a microtubule, kinesins move along the PFs of tubulins, kinesins exhibit rolling motion towards counter-clockwise (CCW) direction due to left-handed helical structure of GMPCPP-microtubule lattice [29, 30]. Therefore, it can be assumed that, in an *in vitro* gliding assay of GMPCPP-microtubules on kinesins, the CCW rolling motion of kinesins along PFs would be reflected in resulting chirality of rotational motion of the GMPCPP-microtubules.

Results and Discussion

To verify our assumption, an *in vitro* gliding assay of GMPCPP-microtubules was demonstrated on a kinesin coated substrate in the presence of methylcellulose (Figure 1) where we varied the density of microtubules over a wide range. As shown by the fluorescence microscopy images (Figure 2a, b), microtubules exhibited translational motion at low density. Upon increasing the density, the microtubules started to rotate in CCW direction which indicated chirality in their (rotational) motion (Figure 2a, c). In order to evaluate the chirality in motion of the microtubules, Left/right asymmetry (LR asymmetry) of microtubules trajectory was analyzed by tracking the moving direction of individual microtubules and measuring the rotational angle (θ) of the microtubules with respect to a reference axis. Preferential motion of the microtubules either in the CW or CCW direction was defined by the positive or negative values of the cosine of rotational angle respectively (Figure 2e). The cosine of the rotational angles of microtubules were then plotted against the density of microtubules to understand the LR asymmetry in microtubule motion. From the analysis, it can be confirmed that, at low density the microtubules exhibited translational motion with a slight tendency to rotate in the CCW direction without any preference in their global orientation. The cosine of rotational angle of microtubules exhibit less negative values (almost 25%) in the range of (-0.007) to (-0.7) (Figure 2e). Increase in the microtubule density above 1.4 $x10^5/mm^2$ facilitated emergence of local monopolar flocks embedded in the homogeneous disordered microtubule regime (Figure 2a, Movie S1). These moving flocks showed distinct CCW rotational motion. As shown in Figure 2e, at relatively high density the cosine values of rotational angles of microtubules become negative in the range of (-0.05) to (-0.8). This implies that the gliding microtubules tend to skew to the CCW direction as the density of microtubules increases. With further increase in the density of microtubules, a large-scale spiral pattern of microtubules rotating in CCW direction emerged (Figure 2d, Movie S2). Apparently, at high density, most of

the microtubules (~84%) rotated towards CCW direction with only a few moving in the CW direction.

The polarity of microtubules, which confirms the degree of monopolar alignment in the flocks, was also analyzed at various densities from the trajectory analysis of the microtubules. Figure 2f shows the correlation between the microtubules density and polarity. From the figure, it is evident that upon increasing the density of microtubules the polarity increases; the monopolar motion of microtubules can be confirmed particularly at the high densities. To further confirm the involvement of intrinsic chirality of microtubules in their monopolar motion, we demonstrated collective motion of the taxol-stabilized GDP microtubules which are mostly of non-chiral lattice structure (~50%). The polarity of microtubules was measured at the density of 2.8 $x10^5/mm^2$. Unlike the GMPCPP microtubules, the polarity of the GDP microtubules was close to 0, which agrees to our previous report [17] This result confirms that the intrinsic charity of microtubules plays the key role in the emergence of monopolar motion at high densities. It is to note that, the unipolar flocking of microtubules was observed particularly at the center of the spiral pattern; at the periphery, the microtubules were found to maintain a bipolar alignment (Figure S1).

The rotational monopolar flocking of microtubules coincides well with the results predicted by our previous *in silico* work. The density-dependent emergence of chiral collective motion of microtubules might be related to a torque generated upon collision of the chiral microtubules. We hypothesize that the collision between microtubules is likely to cause short-term pinning of the motion of microtubules at their front ends (Figure 3a). The pinning of the microtubules at their front ends leads to bending of the front part of the microtubules, which then spreads towards the lagging end of the microtubules to release the local bending stress. More precisely, the left-handed supertwist of microtubules tends to cause leftward bending of the front end which results in rotation of the microtubules in the CCW direction.

To verify our hypothesis experimentally, we demonstrated an *in vitro* gliding assay of microtubules on a substrate with a micro wall made of acrylic resin (Figure 3b, c). The purpose of this experiment was to use the micro wall as an obstacle for the gliding microtubules and to observe the behavior at the front end of the microtubules after the microtubules collide with the wall. Focusing on the microtubules that collided with the wall perpendicularly, we found that ~66.7%

of the microtubules were bent in a CCW direction upon collision and after the collision the microtubules kept moving along the wall (Figure 3d, Movie S3). Interestingly, some of the microtubules which collided with the wall at an acute angle (~30º) moved to the CW direction along the wall after collision and remained stationary for a while (Figure 3e). The microtubules then turned to the CCW direction using their leading tip as the center of the rotational axis, and then continued to move along the wall towards the CCW direction. Such preferential CCW rotation of microtubules mediated by collision with the wall may also happen when the microtubules collide with each other. The observed collision induced CCW motion of microtubules should be amplified with the increase in frequency of the collision event at the high microtubule density conditions. Thus, the torque generated by the microtubules with intrinsic left-handed supertwist lattice gives rise to the CCW rotational motion of individual microtubules and microtubules moving in the groups.

In summary, we show that the kinesin-propelled microtubules with chiral structure self-organize into monopolar flocks that exhibit rotational motion towards CCW direction. Relatively high density of microtubules favors the formation of the large spiral pattern. The observed monopolar flocking of the chiral microtubules, i.e. the GMPCPP-microtubules is different from the bipolar laning of taxol-stabilized GDP microtubules reported in our previous work [17, 18]. The taxol-stabilized GDP microtubules consist of almost an equal proportion of microtubules formed from 13 and 14 protofilaments (PFs) with straight and helical orientation respectively [15, 28]. On the other hand, ~96% of GMPCPP microtubules have helical conformation due to formation of microtubules from 14 PFs [28]. Thus, our results suggest that the collective behavior of microtubules can be controlled simply by tuning the proportion of chiral microtubules for any population.

From the gliding behavior of the single microtubules colliding with the micro wall, we speculate that the observed preferential motion of monopolar flocks towards CCW direction arises due to the bending of the microtubules (twisted by surface immobilized kinesins) due to collision among the microtubules. The observed bias in motion of microtubules towards CCW direction is similar to the "Interaction torque" (IT) reported in our previous *in silico* work [27]. However, at this moment, any correlation between the density of microtubules and emergence of monopolar flocks is unclear from the outcomes of our wet experiments.

Our previously reported simulation suggests that IT also induces anisotropy in the system. When the microtubules moving in opposite directions collide, the bias towards CCW direction may force microtubules to move apart from each other (Figure S2). Intrinsic CCW rotation of single microtubules may also play a role in this repulsion. On the other hand, if the microtubules moving in the same direction collide, their moving direction is not changed which may facilitate the formation of monopolar flocks. Although this model may explain the mechanism of monopolar flocking at the center of the spiral, it doesn't satisfy the bipolar alignment of microtubules observed at the periphery of the spiral pattern. This unique coexisting ordered states of mono- and bi-polar alignment was previously reported in the *in vitro* gliding assay of F-actins driven by myosin [31]. The interesting aspect of our results is that the coexistence of two ordered states seems to be related to the geometry of the microtubule pattern, such as the curvature of their moving trajectory. In addition, the lifetime of each state is longer (several hours) than what was reported for the actin myosin system. In depth study, based on experiments and simulations, will be performed in future in order to understand the detail mechanism of polar flocking of microtubules. This work will help understand how the chirality of self-propelled objects influences their global chiral behavior in collective motion and facilitates the emergence of large-scale chiral structures [32-36]. Spontaneous emergence of unidirectional motion of motile objects in the absence of external force [21-25] and ratchet systems [26] will widen the applications of self-propelled systems in nanotechnology.

Acknowledgement

This work is supported by JSPS KAKENHI grant number 20K15141 (to D.I), JP16K17777, JP19K03764 (to T.H), JP19H01863, JP19K03772, JP18K03555, JP16K05512 (to R.A) and JP18H03673 (to A.K); Mechanobiology Institute, National University of Singapore, (to T.H); a research grant from Hirose Foundation to A.M.R.K (PK22201017); a Grant-in-Aid for Scientific Research on Innovative Areas "Molecular Engine" (JSPS KAKENHI Grant Number JP18H05423), a Grant-in-Aid for JSPS Research Fellows (18F18323) and New Energy and Industrial Technology Development Organization (NEDO) (JPNP20006) (to A.K); "Leading Initiative for Excellent Young Researchers (LEADER)" (JSPS Grant number RAHJ290002), Kazato Research Encouragement Prize and Nikki-Saneyoshi Scholarship Foundation Grant (to D.I).

Materials and methods

Purification of tubulin and kinesin and labelling of tubulin

A high-concentration PIPES buffer (1 M PIPES, 20 mM EGTA, and 10 mM $MgCl_2$; pH adjusted to 6.8 using KOH) was used to purify tubulin from the porcine brain. To prepare high-concentration PIPES buffer and 80 mM PIPES buffer (BRB80), PIPES from Sigma was used, and KOH was used to adjust the pH [37]. Recombinant kinesin-1 consisting of the first 573 amino-acid residues of human kinesin-1 was prepared by following the purification method reported literature [38]. ATTO-488 labelled tubulin was prepared using ATTO-488 succinimidyl ester (ATTO-488; ATTO-Tec Gmbh) and ATTO-565 labelled tubulin was prepared using ATTO-565 succinimidyl ester (ATTO-565; ATTO-Tec Gmbh) according to the standard techniques [39]. The labelling ratio of both ATTO-488 labelled tubulin and ATTO-565 labelled tubulin was 1.0. The ratio was determined by measuring the absorbance of tubulin, ATTO-488 dye and ATT-565 dye at 280 nm, 501 nm and 564 nm respectively. The labelled tubulin was mixed with non-labelled tubulin at a ratio of 4:1 in a way that the concentration of tubulin in the solution became 70 μM.

Preparation of microtubules

Two types of microtubules were separately prepared by polymerizing ATTO-488 labelled and ATTO-565 labelled tubulin. 70 μM labelled tubulin was incubated at 37 ºC in a polymerization buffer (80 mM PIPES, 1 mM EGTA, 5 mM $MgCl_2$, 1 mM GMPCPP; pH 6.8). The solution containing the microtubules was then diluted with motility buffer (80 mM PIPES, 1 mM EGTA, 2 mM $MgCl_2$, 0.5 mg/mL casein, 1 mM DTT, 10 μM paclitaxel and ~1% DMSO; pH 6.8). The final solution was made by mixing these two different dyes labelled microtubules, such that the ratio of the microtubules would remain 9:1 (ATTO 488: ATTO 565).

In vitro gliding assay of microtubules on a kinesin coated glass substrate

In vitro gliding assay of microtubules was performed as described in literature [17, 18]. An open flow cell with dimensions of 5×5 mm^2 (W×L) was prepared on a 40×50 mm^2 cover glass (MATSUNAMI), without using any spacer or coverslip. The open cell was then plasma treated for 3 min by a plasma etcher (SEDE-GE; Meiwafosis) to make it hydrophilic. Then, 5 μL casein buffer (BRB80 buffer supplemented with 0.5 mg/mL casein) was applied on the flow cell. After incubating for 3 min, the flow cell was washed with 10 μL of motility buffer. Then, 5 μL of 500 nM kinesin solution (~80 mM PIPES, 1 mM EGTA, 1 mM $MgCl_2$, 0.5 mg/mL casein, 1 mM DTT,

10 μM paclitaxel/DMSO, ~1% DMSO; pH 6.8) was introduced and incubated for 5 min. The flow cell was washed with 15 μL of motility buffer. Next, 6 μL of microtubule solution of prescribed concentration was introduced and incubated for 4 min, followed by washing with 15 μL of motility buffer two times. Then, 15 μL of 10 mM ATP buffer (~80 mM PIPES, 1 mM EGTA, 1 mM $MgCl_2$, 0.5 mg/mL casein, 1 mM DTT, 10 μM paclitaxel/DMSO, ~1% DMSO; pH 6.8) supplemented with 0.3 wt% methylcellulose (methylcellulose 4000, Junsei Chemical Co., Ltd, MW=140 kDa) was introduced into the flow cell. All the aforementioned experiments were performed at 25 ºC in an inert nitrogen gas atmosphere [40].

Collision assay with a micro-wall

The micro-wall was fabricated on a cover slip (24 x 60 mm^2) by using UV acrylic hard type resin (REJICO, Japan). To make a smooth surface of the wall, we sandwiched a small water droplet between two coverslips and contacted the edge of the water with the resin. The resin was cured by UV/LED Nail Lamp (wavelength at 365 and 405 nm, 6W) for 45 sec UV exposure. After curing the resin, one of the coverslips was removed and the flow chamber was assembled by using two double-sided tapes as spacers between top small cover slip (18 x 18 mm^2) and the bottom cover slip with the micro-wall. The gliding assay was performed as mentioned above.

Microscopic image capture

The samples were illuminated with a 100W mercury lamp and visualized with an epifluorescence microscope (Eclipse Ti; Nikon) using oil-coupled Plan Apo 40× 1.40 objectives (Nikon). Filter blocks with UV-cut specifications (TRITC: EX540/25, DM565, BA606/55; GFP-B: EX480/30, DM505, BA515; Nikon) were used in the optical path of the microscope to allow for visualization of samples while eliminating the UV portion of the radiation and minimizing the harmful effects of UV radiation on the samples. Images and movies were captured using a cooled CMOS camera (Neo sCMOS and Zyla5.5 for collision assay; Andor) connected to a PC. To capture a field of view for more than several minutes, ND filters (ND16, 6.25% transmittance) were inserted into the illuminating light path of the fluorescence microscope to avoid photobleaching**.**

Data analysis

The detail method of data analysis is given in the supplementary information.

References

[1] T. Vicsek, A question of scale, Nature. 411 (2001) 421. https://doi.org/10.1038/35078161.

[2] T. Vicsek, A. Zafeiris, Collective motion, Phys. Rep. 517 (2012) 71–140 https://doi.org/10.1016/j.physrep.2012.03.004.

[3] J.K. Parrish, S. V. Viscido, D. Grünbaum, Self-organized fish schools: An examination of emergent properties, Biol. Bull. 202 (2002) 296–305. https://doi.org/10.2307/1543482.

[4] I.D. Couzin, J. Krause, N.R. Franks, S.A. Levin, Effective leadership and decision-making in animal groups on the move, Nature. 433 (2005) 513–516. https://doi.org/10.1038/nature03236.

[5] C. Dombrowski, L. Cisneros, S. Chatkaew, R.E. Goldstein, J.O. Kessler, Self-concentration and large-scale coherence in bacterial dynamics, Phys. Rev. Lett. 93 (2004) 2–5. https://doi.org/10.1103/PhysRevLett.93.098103.

[6] J. Palacci, S. Sacanna, A.P. Steinberg, D.J. Pine, P.M. Chaikin, Colloidal Surfers, Science (80-.). 339 (2013) 936–939. http://www.sciencemag.org/content/339/6122/936.full.pdf.

[7] A. Bricard, J.B. Caussin, N. Desreumaux, O. Dauchot, D. Bartolo, Emergence of macroscopic directed motion in populations of motile colloids, Nature. 503 (2013) 95–98. https://doi.org/10.1038/nature12673.

[8] J. Yan, M. Han, J. Zhang, C. Xu, E. Luijten, S. Granick, Reconfiguring active particles by electrostatic imbalance, Nat. Mater. 15 (2016) 1095–1099. https://doi.org/10.1038/nmat4696.

[9] J. Zhang, E. Luijten, B.A. Grzybowski, S. Granick, Active colloids with collective mobility status and research opportunities, Chem. Soc. Rev. 46 (2017) 5551–5569. https://doi.org/10.1039/c7cs00461c.

[10] V. Schaller, C. Weber, C. Semmrich, E. Frey, A.R. Bausch, Polar patterns of driven filaments, Nature. 467 (2010) 73–77. https://doi.org/10.1038/nature09312.

[11] Y. Sumino, K.H. Nagai, Y. Shitaka, D. Tanaka, K. Yoshikawa, H. Chaté, K. Oiwa, Large-scale vortex lattice emerging from collectively moving microtubules, Nature. 483 (2012) 448–452. https://doi.org/10.1038/nature10874.

[12] H. Hess, J. Clemmens, C. Brunner, R. Doot, S. Luna, K.H. Ernst, V. Vogel, Molecular self-assembly of “nanowires” and “nanospools” using active transport, Nano Lett. 5 (2005) 629–633. https://doi.org/10.1021/nl0478427.

[13] V. VanDelinder, S. Brener, G.D. Bachand, Mechanisms Underlying the Active Self-Assembly of Microtubule Rings and Spools, Biomacromolecules. 17 (2016) 1048–1056. https://doi.org/10.1021/acs.biomac.5b01684.

[14] R. Kawamura, A. Kakugo, K. Shikinaka, Y. Osada, J.P. Gong, Ring-shaped assembly of microtubules shows preferential counterclockwise motion, Biomacromolecules. 9 (2008) 2277–2282. https://doi.org/10.1021/bm800639w.

[15] A. Kakugo, A.M.R. Kabir, N. Hosoda, K. Shikinaka, J.P. Gong, Controlled clockwise-counterclockwise motion of the ring-shaped microtubules assembly, Biomacromolecules. 12 (2011) 3394–3399. https://doi.org/10.1021/bm200829t.

[16] S. Wada, A.M.R. Kabir, R. Kawamura, M. Ito, D. Inoue, K. Sada, A. Kakugo, Controlling the bias of rotational motion of ring-shaped microtubule assembly, Biomacromolecules. 16 (2015) 374–378. https://doi.org/10.1021/bm501573v.

[17] D. Inoue, B. Mahmot, A.M.R. Kabir, T.I. Farhana, K. Tokuraku, K. Sada, A. Konagaya, A. Kakugo, Depletion force induced collective motion of microtubules driven by kinesin, Nanoscale. 7 (2015) 18054–18061. https://doi.org/10.1039/c5nr02213d.

[18] A. Saito, T.I. Farhana, A.M.R. Kabir, D. Inoue, A. Konagaya, K. Sada, A. Kakugo, Understanding the emergence of collective motion of microtubules driven by kinesins: role of concentration of microtubules and depletion force, RSC Adv. 7 (2017) 13191–13197. https://doi.org/10.1039/c6ra27449h.

[19] K. Kim, N. Yoshinaga, S. Bhattacharyya, H. Nakazawa, M. Umetsu, W. Teizer, Large-scale chirality in an active layer of microtubules and kinesin motor proteins, Soft Matter. 14 (2018) 3221–3231. https://doi.org/10.1039/c7sm02298k.

[20] S. Tanida, K. Furuta, K. Nishikawa, T. Hiraiwa, H. Kojima, K. Oiwa, M. Sano, Gliding filament system giving both global orientational order and clusters in collective motion, Phys. Rev. E. 101 (2020) 1–15. https://doi.org/10.1103/PhysRevE.101.032607.

[21] S. Hiyama, R. Gojo, T. Shima, S. Takeuchi, K. Sutoh, Biomolecular-motor-based nano- or microscale particle translocations on DNA microarrays, Nano Lett. 9 (2009) 2407–2413. https://doi.org/10.1021/nl901013k.

[22] H. Hess, J. Clemmens, J. Howard, V. Vogel, Surface imaging by self-propelled nanoscale probes, Microsc. Microanal. 8 (2002) 1092–1093. https://doi.org/10.1017/s1431927602103539.

[23] H. Hess, G.D. Bachand, V. Vogel, Powering Nanodevices with Biomolecular Motors, Chem. - A Eur. J. 10 (2004) 2110–2116. https://doi.org/10.1002/chem.200305712.

[24] D. V. Nicolau, M. Lard, T. Korten, F.C.M.J.M. Van Delft, M. Persson, E. Bengtsson, A. Månsson, S. Diez, H. Linke, D. V. Nicolau, Parallel computation with molecular-motor-propelled agents in nanofabricated networks, Proc. Natl. Acad. Sci. U. S. A. 113 (2016) 2591–2596. https://doi.org/10.1073/pnas.1510825113.

[25] D. Inoue, T. Nitta, A.M.R. Kabir, K. Sada, J.P. Gong, A. Konagaya, A. Kakugo, Sensing surface mechanical deformation using active probes driven by motor proteins, Nat. Commun. 7 (2016) 1–10. https://doi.org/10.1038/ncomms12557.

[26] R. Di Leonardo, L. Angelani, D. Dell'Arciprete, G. Ruocco, V. Iebba, S. Schippa, M.P. Conte, F. Mecarini, F. De Angelis, E. Di Fabrizio, Bacterial ratchet motors, Proc. Natl. Acad. Sci. U. S.

A. 107 (2010) 9541–9545. https://doi.org/10.1073/pnas.0910426107.

[27] T. Hiraiwa, R. Akiyama, D. Inoue, A.M.R. Kabir, A. Kakugo, Mono-polar clustering of self-propelled particles through left-right asymmetry, (2021) 1–11. http://arxiv.org/abs/2101.02130.

[28] A.A. Hyman, D. Chretien, I. Arnal, R.H. Wade, Structural changes accompanying GTP hydrolysis in microtubules: Information from a slowly hydrolyzable analogue guanylyl-(α,β)-methylene- diphosphonate, J. Cell Biol. 128 (1995) 117–125. https://doi.org/10.1083/jcb.128.1.117.

[29] B. Nitzsche, F. Ruhnow, S. Diez, Quantum-dot-assisted characterization of microtubule rotations during cargo transport, Nat. Nanotechnol. 3 (2008) 552–556. https://doi.org/10.1038/nnano.2008.216.

[30] S. Ray, E. Meyhöfer, R.A. Milligan, J. Howard, Kinesin follows the microtubule's protofilament axis, J. Cell Biol. 121 (1993) 1083–1093. https://doi.org/10.1083/jcb.121.5.1083.

[31] L. Huber, R. Suzuki, T. Krüger, E. Frey, A.R. Bausch, Emergence of coexisting ordered states in active matter systems, Science (80-.). 361 (2018) 255–258. https://doi.org/10.1126/science.aao5434.

[32] S.R. a. Naganathan, S. Fürthauer, M. Nishikawa, F. Jülicher, S.W. Grill, Active torque generation by the actomyosin cell cortex drives left-right symmetry breaking, Elife. 3 (2014) e04165. https://doi.org/10.7554/eLife.04165.

[33] Y.H. Tee, T. Shemesh, V. Thiagarajan, R.F. Hariadi, K.L. Anderson, C. Page, N. Volkmann, D. Hanein, S. Sivaramakrishnan, M.M. Kozlov, A.D. Bershadsky, Cellular chirality arising from the self-organization of the actin cytoskeleton, Nat. Cell Biol. 17 (2015) 445–457. https://doi.org/10.1038/ncb3137.

[34] M. Novak, B. Polak, J. Simunić, Z. Boban, B. Kuzmić, A.W. Thomae, I.M. Tolić, N. Pavin, The mitotic spindle is chiral due to torques within microtubule bundles, Nat. Commun. 9 (2018). https://doi.org/10.1038/s41467-018-06005-7.

[35] S. Thitamadee, K. Tuchihara, T. Hashimoto, Microtubule basis for left-handed helical growth in Arabidopsis, Nature. 417 (2002) 193–196. https://doi.org/10.1038/417193a.

[36] T. Ishida, Y. Kaneko, M. Iwano, T. Hashimoto, Helical microtubule arrays in a collection of twisting tubulin mutants of Arabidopsis thaliana, Proc. Natl. Acad. Sci. U. S. A. 104 (2007) 8544–8549. https://doi.org/10.1073/pnas.0701224104.

[37] M. Castoldi, A. V. Popov, Purification of brain tubulin through two cycles of polymerization-depolymerization in a high-molarity buffer, Protein Expr. Purif. 32 (2003) 83–88. https://doi.org/10.1016/S1046-5928(03)00218-3.

[38] R.B. Case, D.W. Pierce, N. Hom-Booher, C.L. Hart, R.D. Vale, The directional preference of

kinesin motors is specified by an element outside of the motor catalytic domain, Cell. 90 (1997) 959–966. https://doi.org/10.1016/S0092-8674(00)80360-8.
[39] J. Peloquin, Y. Komarova, G. Borisy, Conjugation of fluorophores to tubulin. Nat Methods. 2 (2005) 299–303. DOI: 10.1038/nmeth0405-299.

[40] A.M.R. Kabir, D. Inoue, A. Kakugo, A. Kamei, J.P. Gong, Prolongation of the active lifetime of a biomolecular motor for in vitro motility assay by using an inert atmosphere, Langmuir. 27 (2011) 13659–13668. https://doi.org/10.1021/la202467f.

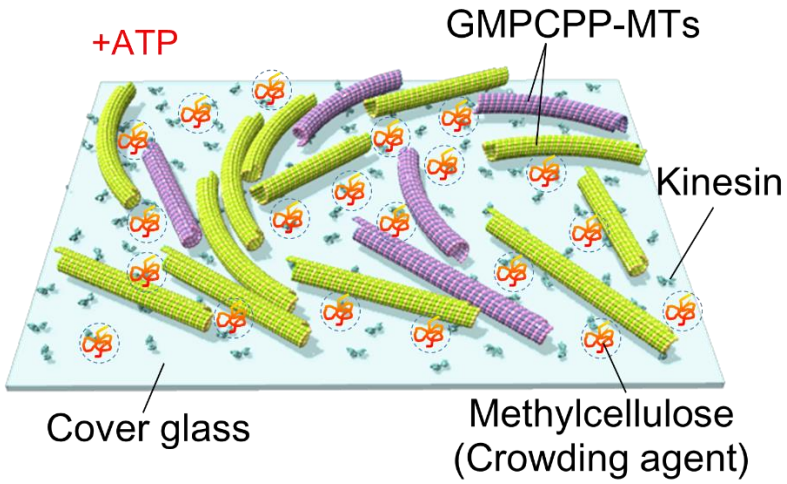

Figure 1. Schematic diagram of an *in vitro* gliding assay of microtubules on a kinesin coated substrate in the presence of methylcellulose.

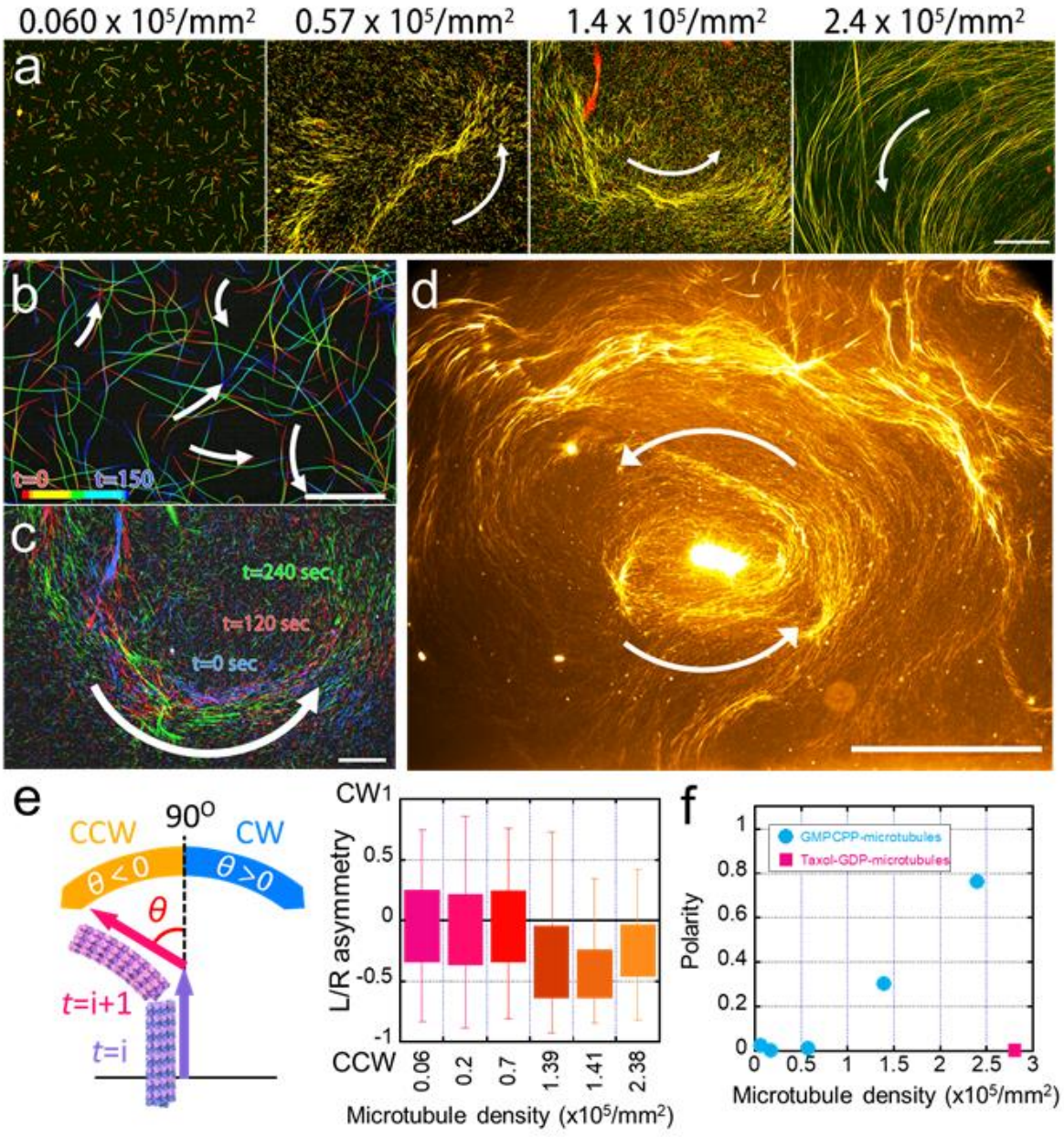

Figure 2. Effect of the density of GMPCPP microtubules on their collective motion. (a) Fluorescence microscopy images of GMPCPP microtubules show emergence of spiral pattern upon increasing the microtubule density. Images were captured after 15 minutes of ATP addition. Arrows indicate the direction of motion of the microtubules. Microtubules form spiral patterns and tend to rotate towards the counter-clockwise direction as the density increases. Kinesin concentration was 500 nM. (b) Temporal color-coded projections of microtubules for 150 second interval frames. (c) Time overlay image of a monopolar microtubule flock rotating to the CCW

direction. (d) The global view of the spiral pattern of GMPCPP microtubules formed at high density conditions. (e) Scheme shows measurement of rotational angle θ of GMPCPP microtubules that was calculated from their trajectory analysis. The initial angle of the microtubules was set as $\theta = 90^{o}$ along their longitudinal axis. When the value of rotational angle was greater than 90^{o} i.e. $\theta > 90^{o}$, it is considered as a positive value which implies clockwise motion of the microtubules. The values of rotational angle that are smaller than 90^{o} i.e. $\theta < 90^{o}$, are considered as negative values which indicates counter-clockwise motion of the microtubules. Box plots show change of LR asymmetry at different densities of microtubules. As the density of microtubules increases most of them tend to move towards the counter-clockwise direction. (f) Change in polarity of GMPCPP upon changing their density. The polarity of microtubules is higher at high density conditions compared to that at the low-density conditions. For comparison, the polarity of taxol-stabilized GDP microtubules is also shown (red square). The experiment was performed as described in a previous work [17]. Scale bars: (a-c) 50 μm and (d) 500 μm.

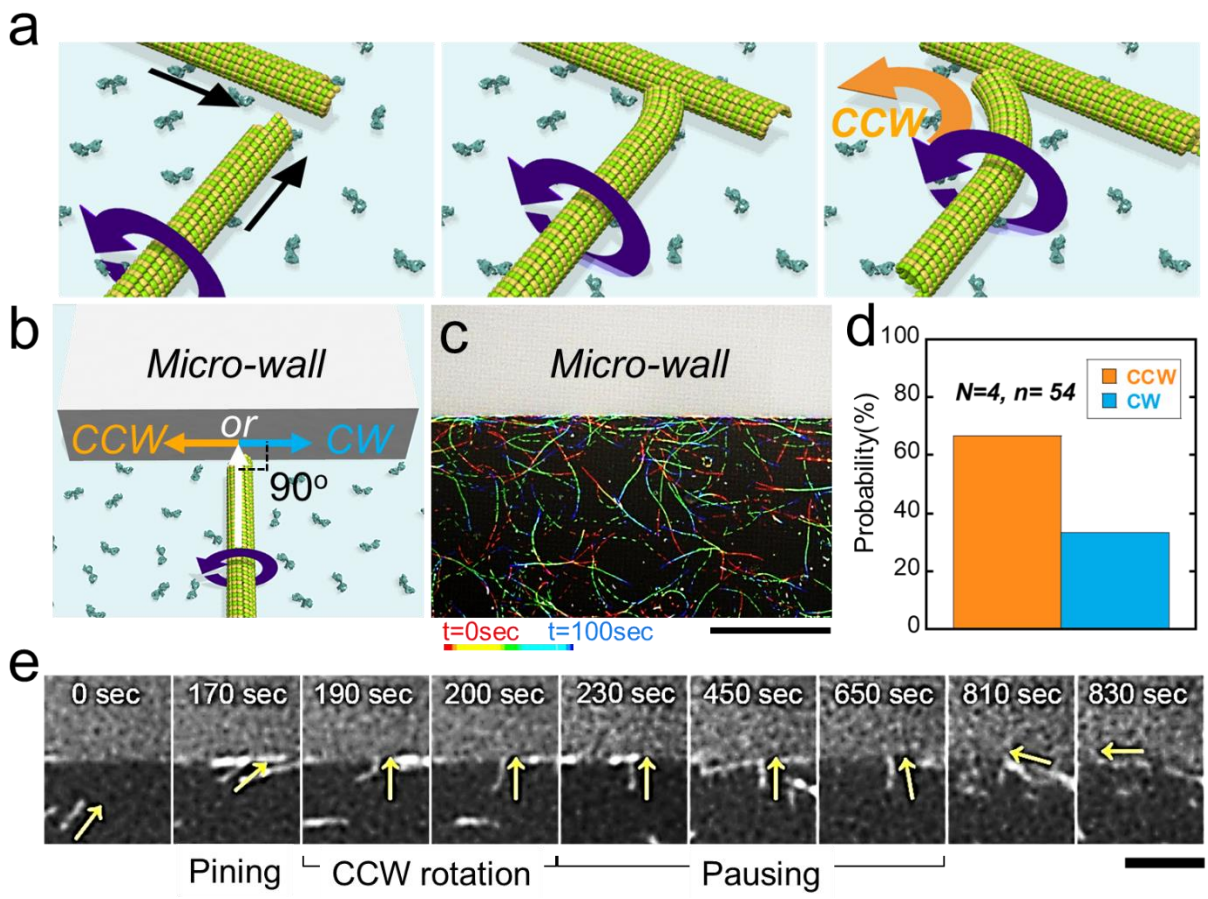

Figure 3. Collision induced preferential CCW rotation of single microtubules. (a) Schematic representation of the model for predicting the CCW rotation of microtubules at high density conditions. Collisions among the neighbor microtubules at high density conditions facilitate rotation of the microtubules towards CCW direction. The black arrows indicate the moving direction of microtubules before collision. (b) Schematic representation of the experimental design for investigating the gliding behavior of microtubules after collision with the micro-wall. (c) Time overlay image shows the trajectory of microtubules near the micro-wall. (d) Probability of CCW or CW rotation of microtubules upon collision with the micro-wall. Only the microtubules which collided with the wall at the angle of 90º were considered for analysis. (e) Time lapse fluorescence microscopy images show a typical example of CCW rotation of a microtubule filament upon collision with the micro wall at an acute angle (~30º) towards CW direction. Scale bars: (c) 25 μm, (e) 10 μm.